LETTER

doi:10.1038/nature20567

Receptor usage dictates HIV-1 restriction by human TRIM5α in dendritic cell subsets

Carla M. S. Ribeiro[1], Ramin Sarrami-Forooshani[1], Laurentia C. Setiawan[1], Esther M. Zijlstra-Willems[1], John L. van Hamme[1], Wikky Tigchelaar[2], Nicole N. van der Wel[2], Neeltje A. Kootstra[1], Sonja I. Gringhuis[1] & Teunis B. H. Geijtenbeek[1]

The most prevalent route of HIV-1 infection is across mucosal tissues after sexual contact. Langerhans cells (LCs) belong to the subset of dendritic cells (DCs) that line the mucosal epithelia of vagina and foreskin and have the ability to sense and induce immunity to invading pathogens[1]. Anatomical and functional characteristics make LCs one of the primary targets of HIV-1 infection[2]. Notably, LCs form a protective barrier against HIV-1 infection and transmission[3–5]. LCs restrict HIV-1 infection through the capture of HIV-1 by the C-type lectin receptor Langerin and subsequent internalization into Birbeck granules[5]. However, the underlying molecular mechanism of HIV-1 restriction in LCs remains unknown. Here we show that human E3-ubiquitin ligase tri-partite-containing motif 5α (TRIM5α) potently restricts HIV-1 infection of LCs but not of subepithelial DC-SIGN$^+$ DCs. HIV-1 restriction by TRIM5α was thus far considered to be reserved to non-human primate TRIM5α orthologues[6–9], but our data strongly suggest that human TRIM5α is a cell-specific restriction factor dependent on C-type lectin receptor function. Our findings highlight the importance of HIV-1 binding to Langerin for the routeing of HIV-1 into the human TRIM5α-mediated restriction pathway. TRIM5α mediates the assembly of an autophagy-activating scaffold to Langerin, which targets HIV-1 for autophagic degradation and prevents infection of LCs. By contrast, HIV-1 binding to DC-SIGN$^+$ DCs leads to disassociation of TRIM5α from DC-SIGN, which abrogates TRIM5α restriction. Thus, our data strongly suggest that restriction by human TRIM5α is controlled by C-type-lectin-receptor-dependent uptake of HIV-1, dictating protection or infection of human DC subsets. Therapeutic interventions that incorporate C-type lectin receptors and autophagy-targeting strategies could thus provide cell-mediated resistance to HIV-1 in humans.

HIV-1 restriction by Langerin occurs after HIV-1 fusion but before integration of viral DNA into the host genome[10]. Therefore, we investigated the role of TRIM5α, as this E3-ubiquitin ligase is a host restriction factor that restricts retroviruses after fusion by binding incoming retroviral capsid and interfering with the uncoating and reverse-transcription processes[6,11–13]. We used both primary human LCs and human MUTZ3-derived LCs (MUTZ-LCs). Langerin on MUTZ-LCs[14], as on primary LCs[5], controls HIV-1 restriction mechanisms (Extended Data Fig. 1a–e). Notably, silencing of TRIM5α in human LCs by RNA interference (Extended Data Fig. 2a, b, h) resulted in increased viral integration and infection with both CXCR4- and CCR5-tropic viruses, as well as increased HIV-1 transmission to activated CD4$^+$ T cells (Fig. 1a–e, Extended Data Fig. 3a, b). These data strongly suggest that human TRIM5α is a potent restriction factor for HIV-1 in LCs.

We next investigated the molecular mechanism of human TRIM5α restriction and the interplay with autophagy machinery, as the latter has been implicated in the function of TRIM molecules[15]. At steady-state, human TRIM5α associated in LCs with autophagosomal molecule Atg16L1 and adaptor protein p62 (Extended Data Fig. 4a). Atg16L1 not only binds to ubiquitin-decorated cargos but also forms large protein complexes with Atg5 and Atg12 to elicit autophagosome biogenesis by building protein scaffolds as well as mediating expansion of autophagosomes[16,17]. Notably, HIV-1 infection of LCs increased Atg5 recruitment to TRIM5α–Atg16L1–p24 capsid complexes (Fig. 2a). These data suggest that human TRIM5α in LCs is involved in the assembly of core autophagic factors into autophagosome formation upon recruitment of HIV-1 p24 capsid. Notably, HIV-1 infection of LCs increased the number of autophagosomes (bi- or multilamellar vesicles) compared to uninfected LCs (Fig. 2b, c). Furthermore, although HIV-1 infection alone did

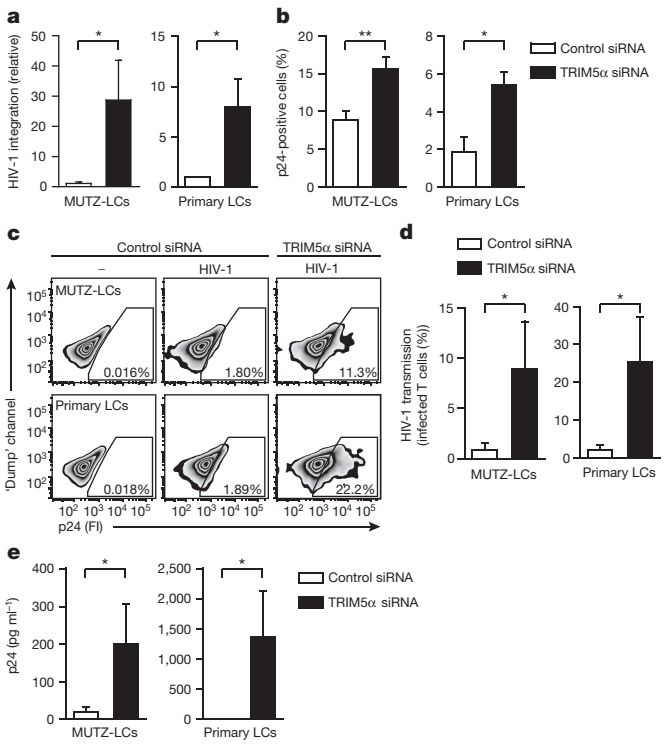

Figure 1 | Human TRIM5α is a restriction factor for HIV-1 in LCs. **a**, **b**, HIV-$1_{NL4.3}$ integration (**a**) and infection (**b**) of MUTZ-LCs and primary LCs after TRIM5α silencing, determined by Alu-PCR (**a**) and intracellular p24 staining (**b**). siRNA, small interfering RNA. **c**–**e**, HIV-1_{SF162} transmission by MUTZ-LCs and primary LCs after TRIM5α silencing, determined in LC–T-cell coculture by intracellular p24 staining (**c** (representative of $n = 4$), **d**) and p24-antigen ELISA (**e**). FI, fluorescence intensity. $^*P < 0.05$, $^{**}P < 0.01$ (two-tailed t-test). Data are mean ± s.d. of four (**a**, MUTZ-LCs), three (**a** (primary LCs), **b**) and four (**d**, **e**) independent experiments.

[1]Department of Experimental Immunology, Academic Medical Center, University of Amsterdam, Meibergdreef 9, 1105 AZ Amsterdam, The Netherlands. [2]Department of Cell Biology & Histology, Academic Medical Center, University of Amsterdam, Meibergdreef 9, 1105 AZ Amsterdam, The Netherlands.

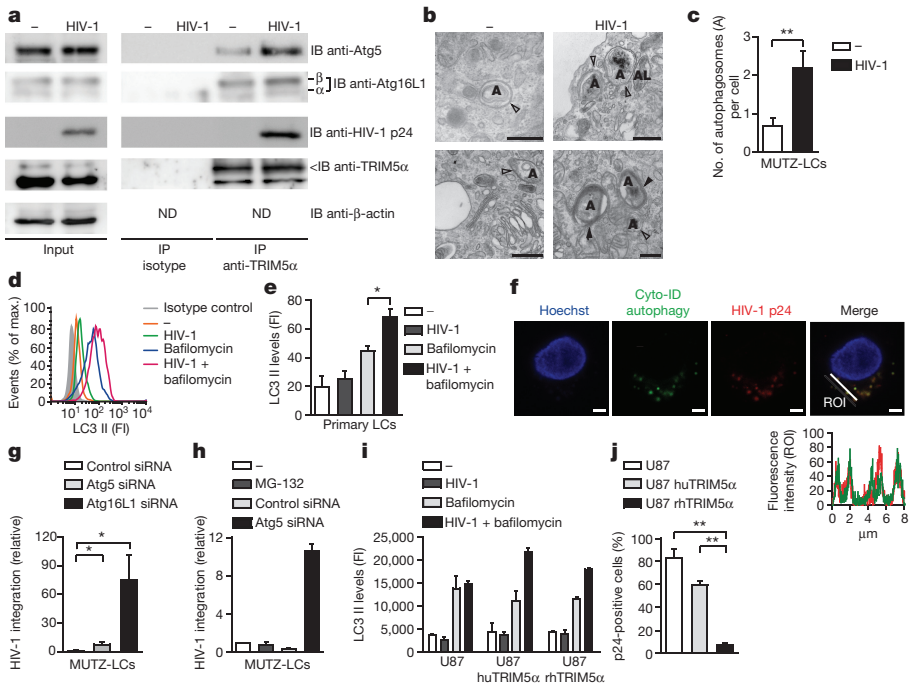

Figure 2 | Autophagy restricts HIV-1 infection of LCs. a, Atg5, Atg16L1, HIV-1 p24 and TRIM5α in whole-cell lysates of MUTZ-LCs infected with HIV-$1_{NL4.3}$ before (input) or after immunoprecipitation (IP) with TRIM5α, determined by immunoblotting (IB); representative of $n = 3$. ND, not determined. For gel source data, see Supplementary Fig. 1. **b**, **c**, Electron microscopy analyses for bi- (empty arrowheads) and multi-lamellar autophagosomes (filled arrowheads) in HIV-$1_{NL4.3}$-infected MUTZ-LCs. A, autophagosomes; AL, autolysosomes. Scale bar, 500 nm. Representative of $n = 3$ (**b**); mean ± s.d., $n = 50$ images per condition (**c**). **d**, **e**, Autophagy induction in primary LCs pre-treated with bafilomycin followed by incubation with HIV-$1_{NL4.3}$, determined by intracellular LC3 II levels (representative of $n = 3$ (**d**)). **f**, Confocal microscopy analyses of primary LCs infected with HIV-$1_{NL4.3}$. Scale bars, 2.5 μm. Histogram of Cyto-ID and p24 fluorescence intensities (ROI, region of interest; representative of $n = 2$). **g**, **h**, HIV-$1_{NL4.3}$ integration into MUTZ-LCs after Atg5 or Atg16L1 silencing or after pre-treatment with MG-132, determined by Alu-PCR. **i**, Autophagy induction in U87 cells or transduced with human or rhesus TRIM5α pre-treated with bafilomycin followed by incubation with HIV-1_{SF162}, determined by intracellular LC3 II levels ($n = 2$). **j**, HIV-1_{SF162} infection of U87 transfectants, determined by intracellular p24 staining. $*P < 0.05$, $**P < 0.01$ (two-tailed *t*-test). Data are mean ± s.d. of three (**e**, **h**, **j**) and four (**g**) independent experiments.

not affect microtubule-associated protein light chain 3 II (LC3 II) levels compared to uninfected cells, these levels were increased after pre-treatment with lysosomal inhibitor bafilomycin of HIV-1-infected cells (Fig. 2d, e, Extended Data Fig. 4b). These data indicate that HIV-1 increases autophagic flux in LCs, rather than blocking autophagic maturation.

Therefore, we investigated whether autophagy restricts HIV-1 infection in LCs. HIV-1 p24 capsid co-immunoprecipitated with autophagic molecules (Fig. 2a) and we observed targeting of HIV-1 p24 capsid into autophagic vesicles in LCs (Fig. 2f). Notably, silencing of Atg5 or Atg16L1 increased both HIV-1 integration and infection of LCs (Fig. 2g, h, Extended Data Figs 2a, i, j, 4c). Similarly, an increase of HIV-1 integration was observed after silencing Atg13 or FIP200 (Extended Data Fig. 4d), suggesting that the ULK1-dependent autophagy pathway prevents infection of LCs. Enhancing autophagy-mediated lysis by rapamycin decreased HIV-1 integration in primary LCs and led to degradation of HIV-1 p24 in primary LCs (Fig. 3a–c, g). Collectively, these data strongly suggest that, upon viral fusion, HIV-1 capsids are targeted into autophagosomes for lysosomal degradation. Furthermore, silencing of Atg5 in TRIM5α-silenced LCs did not further affect either HIV-1 integration or infection, supporting the notion that the mechanism of TRIM5α restriction is dependent on Atg5 function (Extended Data Fig. 2d, e, 4e, f). The role for TRIM5α in autophagy activation was further supported by our data showing that HIV-1 infection of $CD4^+CCR5^+$ U87 cells that overexpressed either human or rhesus TRIM5α increased Atg5 recruitment to Atg16L1–TRIM5α complexes (Extended Data Fig. 5a), and increased LC3 II levels in the presence of bafilomycin (Fig. 2i, Extended Data Fig. 5b). In line with previous reports[6,7,11,15], rhesus but not human TRIM5α strongly restricted HIV-1 infection (Fig. 2j). Thus, human TRIM5α is unable to restrict HIV-1 infection in U87 cells despite induction of autophagy upon HIV-1 infection. Therefore, we hypothesized that LC-specific uptake through Langerin might drive efficient human TRIM5α restriction. As vesicular stomatitis virus-G glycoprotein (VSV-G)-pseudotyped viruses do not interact with Langerin[18] and infect cells through endocytosis-mediated uptake independently of CD4 and CCR5, we silenced endogenous TRIM5α in LCs and infected them with HIV-1 isolate NL4.3 or VSV-G-pseudotyped NL4.3(ΔEnv) HIV-1. Silencing of human TRIM5α in LCs increased integration of HIV-1, but notably not of VSV-G-pseudotyped HIV-1 (Fig. 3d). These findings strongly suggest that human TRIM5α restriction depends on the virus uptake route through Langerin. Therefore, we investigated whether Langerin is part of the TRIM5α–autophagy complex. Atg16L1 and TRIM5α co-immunoprecipitated with Langerin in LCs at both steady state and after HIV-1 exposure (Fig. 3e). Confocal microscopy confirmed the partial colocalization of human TRIM5α and Langerin in primary LCs (Fig. 3f). These data suggest that Langerin couples HIV-1 routeing to human TRIM5α-mediated autophagic restriction. Notably, although rapamycin, which induces autophagy, alone did not affect Langerin expression, HIV-1 infection strongly decreased Langerin levels independently of rapamycin (Fig. 3g). We could also detect the presence of Birbeck granules within autophagosomes in LCs by electron microscopy (Fig. 3h, i). These findings suggest that autophagy machinery intersects with Langerin internalization pathway, and vesicles as well as whole Birbeck granules containing Langerin–HIV-1 capsid complexes are turned over by autophagy upon viral fusion in LCs.

Notably, ectopic expression of Langerin in $CD4^+CCR5^+$ U87 cells strongly restricted HIV-1 integration and infection (Fig. 3j–l), and silencing of either TRIM5α or Atg16L1 in these Langerin-expressing

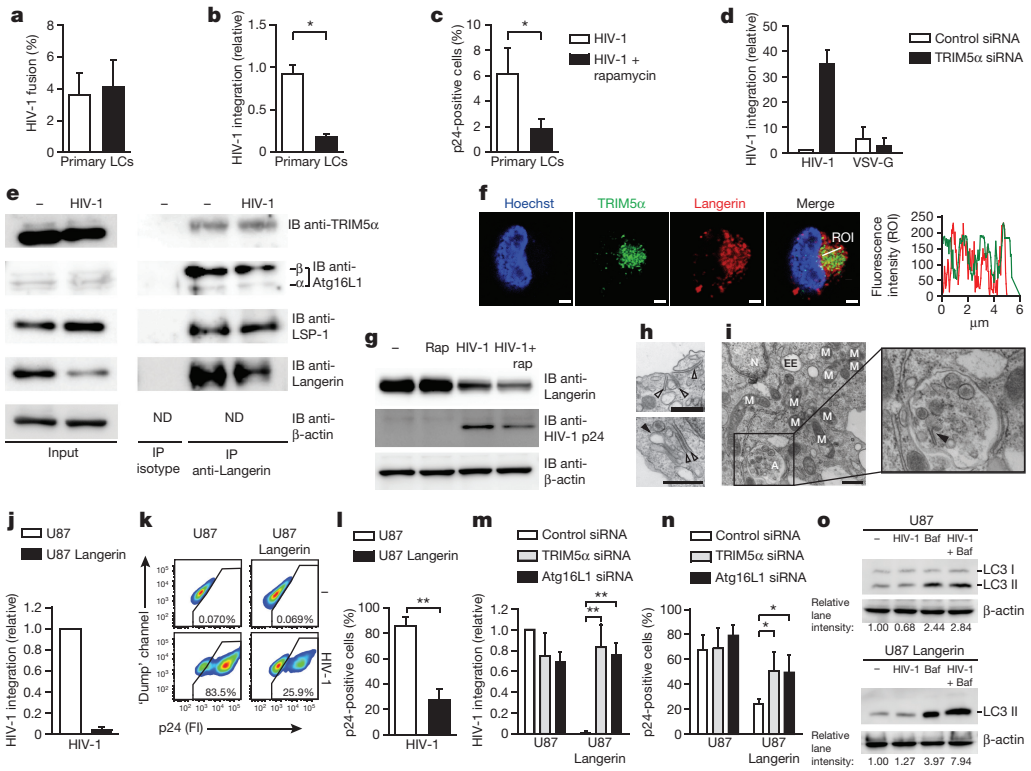

Figure 3 | HIV-1 uptake by Langerin drives human TRIM5α restriction. **a–c**, Primary LCs pre-treated with rapamycin, HIV-$1_{NL4.3-BlaM-Vpr}$ fusion, determined by β-lactamase-Vpr (BlaM-Vpr) assay (**a**), HIV-$1_{NL4.3}$ integration, determined by Alu-PCR (**b**), HIV-$1_{NL4.3}$ infection, determined by intracellular p24 staining (**c**). **d**, HIV-$1_{NL4.3}$ or VSV-G-pseudotyped HIV-$1_{NL4.3}$ integration into MUTZ-LCs after TRIM5α silencing, determined by Alu-PCR ($n = 2$). **e**, TRIM5α, Atg16L1, LSP-1 and Langerin in whole-cell lysates of MUTZ-LCs infected with HIV-$1_{NL4.3}$ before (input) or after immunoprecipitation with Langerin, determined by immunoblotting (representative of $n = 3$). For gel source data, see Supplementary Fig. 1. **f**, Confocal microscopy analyses of primary LCs. Scale bars, 2.5 μm. Histogram of Langerin and TRIM5α fluorescence intensities (ROI, region of interest). **g**, Langerin and HIV-p24 in primary LCs pre-treated with rapamycin followed by incubation with HIV-$1_{NL4.3}$, determined by immunoblotting. **h**, **i**, Electron microscopy analyses for tubular-shaped (empty arrowheads) and racket- shaped (filled arrowheads) Birbeck granules in MUTZ-LCs after incubation with HIV-$1_{NL4.3}$. Scale bars, 500 nm (**i**; original magnification, 2.5× (inset)). EE, early endosomes; M, mitochondria; N, nucleus. Representative of $n = 2$ (**f–i**). **j–l**, HIV-$1_{NL4.3-BaL}$ integration (**j**) or infection (**k**, **l**) of U87 or Langerin$^+$ U87 cells, determined by Alu-PCR (**j**) and intracellular p24 staining (**k** (representative of $n = 4$), **l**). **m**, **n**, HIV-$1_{NL4.3-BaL}$ integration (**m**) and infection (**n**) of U87 transfectants after Atg16L1 or TRIM5α silencing, determined by Alu-PCR (**m**) and intracellular p24 staining (**n**). **o**, Autophagy induction in U87 transfectants pre-treated with bafilomycin followed by incubation with HIV-1_{SF162}, determined by immunoblotting for LC3. Relative abundance of LC3II determined by normalizing to β-actin, representative of $n = 2$. $^*P < 0.05$, $^{**}P < 0.01$ (two-tailed t-test). Data are mean ± s.d. of four (**a**, **l**, **n**) and three (**b**, **c**, **j**, **m**) independent experiments.

U87 cells abrogated restriction (Extended Data Fig. 2f, Fig. 3m, n). Furthermore, increased levels of the TRIM5α–Atg5 complexes co-immunoprecipitated with Atg16L1 and correlated with increased levels of LC3 II upon HIV-1 infection in Langerin-expressing U87 cells, but not in the U87 parental cells (Extended Data Fig. 6a, Fig. 3o). Silencing of human TRIM5α decreased HIV-induced autophagy in Langerin-expressing U87 cells (Extended Data Fig. 6b), which supports the role for TRIM5α in mediating Langerin-dependent autophagic restriction of HIV-1.

We next investigated whether other HIV-1-binding C-type lectin receptors, such as DC-SIGN, can also recruit TRIM5α machinery. DC-SIGN, in contrast to Langerin on LCs, facilitates HIV-1 infection of and transmission by DCs[19,20]. Silencing of TRIM5α in DC-SIGN$^+$ DCs (Extended Data Fig. 2c) affected neither HIV-1 integration nor infection levels of both CXCR4- and CCR5-tropic viruses (Fig. 4a–c, Extended Data Fig. 3c, d). Furthermore, HIV-1 downregulated autophagy in DCs (Fig. 4d), as reported previously[21]. Notably, although TRIM5α co-immunoprecipitated with an antibody against DC-SIGN at steady-state conditions, HIV-1 infection in DCs led to dissociation of TRIM5α from the cytoplasmic domain of DC-SIGN (Fig. 4e). These data underscore that human TRIM5α is a cell-specific restriction factor and support the hypothesis that other C-type lectin receptors also recruit TRIM5α, but only Langerin seems to have the ability to restrict HIV-1 infection through TRIM5α.

To further identify the molecular determinants of TRIM5α restriction, we transduced U87 cells with Langerin(W264R) mutant, which contains a naturally occurring polymorphism within the binding pocket of the extracellular carbohydrate-recognition domain of Langerin and is unable to bind sugars[22]. The Langerin(W264R) mutant did not bind HIV-1 and was unable to restrict HIV-1 infection in U87 cells (Fig. 4f–h), demonstrating that binding to the carbohydrate-recognition domain of Langerin is required for efficient TRIM5α restriction. We have previously shown that differential binding of specific signalling molecules to the cytoplasmic domain of DC-SIGN through adaptor protein LSP-1 dictates intracellular signalling[23]. Similar to DC-SIGN (Fig. 4e), Langerin also interacted with LSP-1 (Fig. 3e)[24]. LSP-1 forms a complex with Langerin, TRIM5α and the autophagosomal molecule Atg16L1 in LCs (Fig. 3e). Immunoprecipitation analyses confirmed the interaction between TRIM5α and LSP-1 in LCs (Extended Data Fig. 6c). Silencing of LSP-1, but not Atg16L1, decreased Langerin binding to TRIM5α (Fig. 4i, Extended Data Fig. 6d). Remarkably, HIV-1 binding to the extracellular carbohydrate-recognition domain of either Langerin or DC-SIGN dictates TRIM5α assembly to the intracellular domain of the C-type lectin-receptor through LSP-1, leading to HIV-1 restriction or infection, respectively. The LC-specific restriction mechanism identified in our study not only highlights the natural barrier function of the mucosa to HIV-1, but also outlines a novel receptor-controlled TRIM5α restriction mechanism.

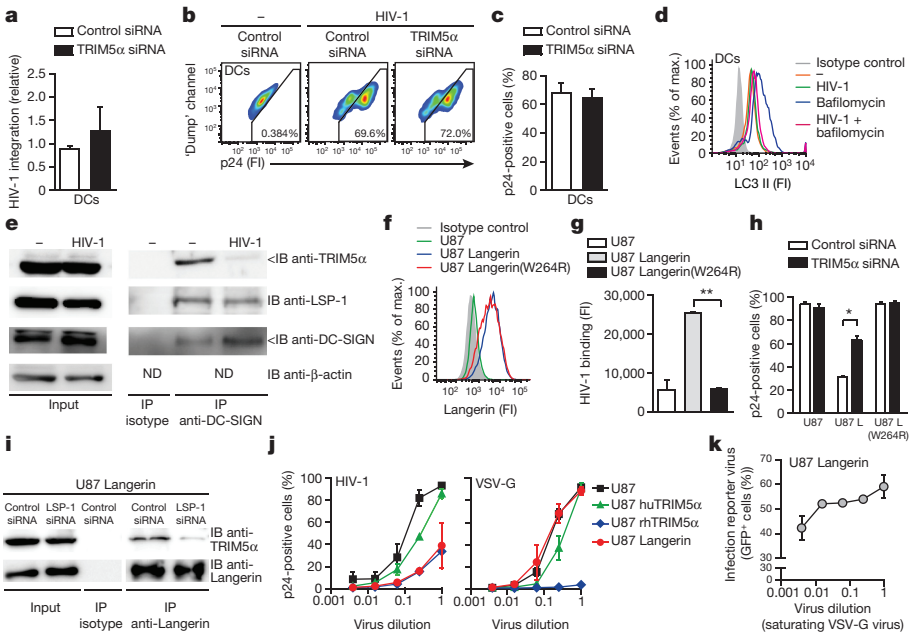

Figure 4 | Human TRIM5α is a cell-specific restriction factor for HIV-1. **a**–**c**, HIV-$1_{NL4.3\text{-}BaL}$ integration (**a**) and infection (**b**, **c**) of DCs after TRIM5α silencing, determined by Alu-PCR (**a**) and intracellular p24 staining (**b** (representative of $n = 6$), **c**). **d**, Autophagy induction in DCs pre-treated with bafilomycin followed by incubation with HIV-$1_{NL4.3\text{-}BaL}$, determined by intracellular LC3 II levels (representative of $n = 2$). **e**, TRIM5α, LSP-1 and DC-SIGN in whole-cell lysates of DCs infected with HIV-$1_{NL4.3\text{-}BaL}$ before (input) or after immunoprecipitation together with DC-SIGN, determined by immunoblotting (representative of $n = 3$). For gel source data, see Supplementary Fig. 1. **f**, Langerin expression in U87 parental cells or transduced with either Langerin or Langerin(W264R) mutant, determined by flow cytometry, representative of $n = 3$. **g**, HIV-1 binding to U87 transfectants, determined by gp120 beads-binding assay. **h**, HIV-$1_{NL4.3\text{-}BaL}$ infection of U87 transfectants after TRIM5α silencing, determined by intracellular p24 staining. **i**, TRIM5α and Langerin in whole-cell lysates of U87 Langerin transfectant after LSP-1 silencing before (input) or after immunoprecipitation together with Langerin, determined by immunoblotting, representative of $n = 2$. **j**, HIV-$1_{NL4.3\text{-}BaL}$ or VSV-G-pseudotyped HIV-1 infection of U87 transfectants, determined by intracellular p24 staining. **k**, Abrogation of restriction in U87 Langerin transfectant after pre-incubation with increasing doses of VSV-G-pseudotyped particles followed by infection with HIV-$1_{NL4.3eGFP\text{-}BaL}$ reporter virus (**j**, **k**; $n = 2$). $^*P < 0.05$, $^{**}P < 0.01$ (two-tailed t-test). Data are mean ± s.d. of three (**a**, **g**, **h**) and six (**c**) independent experiments.

We next compared the restriction mechanism of human TRIM5α in Langerin-expressing U87 cells with that described for rhesus TRIM5α; the two mechanisms seem to differ as silencing of Atg16L1 only relieved rhesus TRIM5α-induced restriction twofold (Extended Data Figs 2g, 5c). In accordance with a previous study[25], proteasome inhibition with MG-132 rescued reverse transcription, but not infection, of U87 cells transduced with rhesus TRIM5α (Extended Data Fig. 7a, b). By contrast, MG-132 did not abrogate HIV-1 restriction in MUTZ-LCs or in Langerin-expressing U87 cells (Fig. 2h, Extended Data Fig. 7c, d). These data further support that restriction by the Langerin-mediated TRIM5α mechanism depends on autophagy machinery and differs from the proteasome-dependent restriction by rhesus TRIM5α. These findings challenge the current hypothesis that human TRIM5α cannot restrict HIV-1 infection[6,7,26,27], although they suggest a mechanism that is distinct from that of rhesus TRIM5α. We next investigated whether the viral envelope affects restriction. Rhesus TRIM5α restricts both HIV-1- and VSV-G-pseudotyped viruses (Fig. 4j), in accordance with previous reports[27,28]. Notably, our data show that the Langerin-controlled human TRIM5α mechanism restricts infection of HIV-1 at the same magnitude as rhesus TRIM5α, but does not restrict infection of VSV-G-pseudotyped virus (which bypasses Langerin uptake). These findings indicate that TRIM5α in human cells, in contrast to rhesus TRIM5α[6], depends on the virus uptake route by Langerin. Furthermore, our data show that TRIM5α restriction in U87 cells transduced with Langerin is saturated by increasing doses of viral capsids, thus rendering cells permissive to infection by a HIV-1 reporter virus (Fig. 4k), as previously shown for rhesus TRIM5α[29,30]. As VSV-G-pseudotyped virus induced autophagy at saturating conditions (Extended Data Fig. 6e), these data strongly suggest that autophagy induction alone does not mediate human TRIM5α-dependent restriction of HIV-1 (Fig. 2i, j, 4k, Extended Data Fig. 6e), but that it requires the formation of a complex between HIV-1 p24 capsid, human TRIM5α and autophagy molecules for restriction (Figs 2a, 4k, Extended Data Fig. 8). Further studies are required to investigate whether direct interaction between human TRIM5α and HIV-1 p24 capsid is required for the Langerin-mediated TRIM5α restriction mechanism. Our data demonstrate that restriction by human TRIM5α is two-tiered; TRIM5α mediates assembly of the autophagy-activating complexes and at the same time requires HIV-1 uptake by Langerin for efficient routeing of the HIV-1 capsid into TRIM5α-dependent autophagic scaffolds. Our study establishes that human TRIM5α is a cell-specific restriction factor for HIV-1 and underscores the importance of selective HIV-1 uptake mechanisms and assembly of molecular determinants in driving human TRIM5α-mediated restriction. Novel TRIM5α-based therapies in combination with strategies targeting C-type lectin receptors, LSP-1 or autophagy could thus represent an important alternative to current antiretroviral therapy in acute retroviral exposure.

Online Content Methods, along with any additional Extended Data display items and Source Data, are available in the online version of the paper; references unique to these sections appear only in the online paper.

Received 24 March; accepted 20 October 2016.
Published online 7 December 2016.

1. Banchereau, J. *et al.* Immunobiology of dendritic cells. *Annu. Rev. Immunol.* **18,** 767–811 (2000).
2. Hladik, F. *et al.* Initial events in establishing vaginal entry and infection by human immunodeficiency virus type-1. *Immunity* **26,** 257–270 (2007).
3. Ribeiro, C. M. S., Sarrami-Forooshani, R. & Geijtenbeek, T. B. H. HIV-1 border patrols: Langerhans cells control antiviral responses and viral transmission. *Future Virol.* **10,** 1231–1243 (2015).
4. Sarrami-Forooshani, R. *et al.* Human immature Langerhans cells restrict CXCR4-using HIV-1 transmission. *Retrovirology* **11,** 52 (2014).
5. de Witte, L. *et al.* Langerin is a natural barrier to HIV-1 transmission by Langerhans cells. *Nat. Med.* **13,** 367–371 (2007).

6. Stremlau, M. *et al.* The cytoplasmic body component TRIM5α restricts HIV-1 infection in Old World monkeys. *Nature* **427,** 848–853 (2004).
7. Sawyer, S. L., Wu, L. I., Emerman, M. & Malik, H. S. Positive selection of primate TRIM5α identifies a critical species-specific retroviral restriction domain. *Proc. Natl Acad. Sci. USA* **102,** 2832–2837 (2005).
8. Song, B. *et al.* Retrovirus restriction by TRIM5α variants from Old World and New World primates. *J. Virol.* **79,** 3930–3937 (2005).
9. Sayah, D. M., Sokolskaja, E., Berthoux, L. & Luban, J. Cyclophilin A retrotransposition into TRIM5 explains owl monkey resistance to HIV-1. *Nature* **430,** 569–573 (2004).
10. van den Berg, L. M. *et al.* Caveolin-1 mediated uptake via Langerin restricts HIV-1 infection in human Langerhans cells. *Retrovirology* **11,** 123 (2014).
11. Stremlau, M. *et al.* Specific recognition and accelerated uncoating of retroviral capsids by the TRIM5α restriction factor. *Proc. Natl Acad. Sci. USA* **103,** 5514–5519 (2006).
12. Yap, M. W., Nisole, S. & Stoye, J. P. A single amino acid change in the SPRY domain of human Trim5α leads to HIV-1 restriction. *Curr. Biol.* **15,** 73–78 (2005).
13. Ganser-Pornillos, B. K. *et al.* Hexagonal assembly of a restricting TRIM5α protein. *Proc. Natl Acad. Sci. USA* **108,** 534–539 (2011).
14. de Jong, M. A. *et al.* Mutz-3-derived Langerhans cells are a model to study HIV-1 transmission and potential inhibitors. *J. Leukoc. Biol.* **87,** 637–643 (2010).
15. Mandell, M. A. *et al.* TRIM proteins regulate autophagy and can target autophagic substrates by direct recognition. *Dev. Cell* **30,** 394–409 (2014).
16. Fujita, N. *et al.* Recruitment of the autophagic machinery to endosomes during infection is mediated by ubiquitin. *J. Cell Biol.* **203,** 115–128 (2013).
17. Moreau, K., Ravikumar, B., Renna, M., Puri, C. & Rubinsztein, D. C. Autophagosome precursor maturation requires homotypic fusion. *Cell* **146,** 303–317 (2011).
18. Gramberg, T. *et al.* Interactions of LSECtin and DC-SIGN/DC-SIGNR with viral ligands: differential pH dependence, internalization and virion binding. *Virology* **373,** 189–201 (2008).
19. Geijtenbeek, T. B. *et al.* DC-SIGN, a dendritic cell-specific HIV-1-binding protein that enhances *trans*-infection of T cells. *Cell* **100,** 587–597 (2000).
20. Gringhuis, S. I. *et al.* HIV-1 exploits innate signaling by TLR8 and DC-SIGN for productive infection of dendritic cells. *Nat. Immunol.* **11,** 419–426 (2010).
21. Blanchet, F. P. *et al.* Human immunodeficiency virus-1 inhibition of immunoamphisomes in dendritic cells impairs early innate and adaptive immune responses. *Immunity* **32,** 654–669 (2010).
22. Ward, E. M., Stambach, N. S., Drickamer, K. & Taylor, M. E. Polymorphisms in human Langerin affect stability and sugar binding activity. *J. Biol. Chem.* **281,** 15450–15456 (2006).
23. Gringhuis, S. I., den Dunnen, J., Litjens, M., van der Vlist, M. & Geijtenbeek, T. B. Carbohydrate-specific signaling through the DC-SIGN signalosome tailors immunity to *Mycobacterium tuberculosis*, HIV-1 and *Helicobacter pylori*. *Nat. Immunol.* **10,** 1081–1088 (2009).
24. Smith, A. L. *et al.* Leukocyte-specific protein 1 interacts with DC-SIGN and mediates transport of HIV to the proteasome in dendritic cells. *J. Exp. Med.* **204,** 421–430 (2007).
25. Wu, X., Anderson, J. L., Campbell, E. M., Joseph, A. M. & Hope, T. J. Proteasome inhibitors uncouple rhesus TRIM5α restriction of HIV-1 reverse transcription and infection. *Proc. Natl Acad. Sci. USA* **103,** 7465–7470 (2006).
26. Perez-Caballero, D., Hatziioannou, T., Yang, A., Cowan, S. & Bieniasz, P. D. Human tripartite motif 5α domains responsible for retrovirus restriction activity and specificity. *J. Virol.* **79,** 8969–8978 (2005).
27. Stremlau, M., Perron, M., Welikala, S. & Sodroski, J. Species-specific variation in the B30.2(SPRY) domain of TRIM5α determines the potency of human immunodeficiency virus restriction. *J. Virol.* **79,** 3139–3145 (2005).
28. Song, B. *et al.* The B30.2(SPRY) domain of the retroviral restriction factor TRIM5α exhibits lineage-specific length and sequence variation in primates. *J. Virol.* **79,** 6111–6121 (2005).
29. Shi, J. & Aiken, C. Saturation of TRIM5α-mediated restriction of HIV-1 infection depends on the stability of the incoming viral capsid. *Virology* **350,** 493–500 (2006).
30. Kootstra, N. A., Munk, C., Tonnu, N., Landau, N. R. & Verma, I. M. Abrogation of postentry restriction of HIV-1-based lentiviral vector transduction in simian cells. *Proc. Natl Acad. Sci. USA* **100,** 1298–1303 (2003).

Supplementary Information is available in the online version of the paper.

Acknowledgements We are grateful to the members of the Host Defense group and Laboratory for Viral Immune Pathogenesis (Department of Experimental Immunology, Academic Medical Center, Amsterdam, The Netherlands) for their input and D. Picavet (van Leeuwenhoek Centrum for Advanced Microscopy, Academic Medical Center, Amsterdam, The Netherlands) for technical assistance during confocal experiments. We wish to thank the Boerhaave Medical Centre (Amsterdam, The Netherlands) and A. Knottenbelt (Flevoclinic, Almere, The Netherlands) for the provision of human skin tissues. This work was supported by the Dutch Scientific Organization NWO (VENI 863.13.025 and VICI 918.10.619), Aids Fonds (2010038) and European Research Council (Advanced grant 670424).

Author Contributions C.M.S.R. designed, performed and interpreted most experiments and prepared the manuscript; R.S.F. assisted with the lentiviral transductions and the confocal experiments; L.C.S. assisted with culturing the $CD4^+CCR5^+$ U87 cell lines and with the lentiviral transductions; E.M.Z.W. cultured MUTZ-LCs and helped with immunoblotting; J.L.v.H. assisted with primary cell isolation and silencing experiments; W.T. and N.N.v.d.W. performed the EM microscopy; N.A.K. and S.I.G. helped prepare the manuscript and T.B.H.G. supervised all aspects of the project.

Author Information Reprints and permissions information is available at www.nature.com/reprints. The authors declare no competing financial interests. Readers are welcome to comment on the online version of the paper. Correspondence and requests for materials should be addressed to T.B.H.G. (t.b.geijtenbeek@amc.uva.nl) or C.M.S.R. (c.m.ribeiro@amc.uva.nl).

Reviewer Information *Nature* thanks J. Luban, C. Munz and G. Towers for their contribution to the peer review of this work.

METHODS

Data reporting. No statistical methods were used to predetermine sample size. The experiments were not randomized and the investigators were not blinded to allocation during experiments and outcome assessment.

Donors, cells and inhibitors. Human skin tissue was obtained from healthy donors undergoing corrective breast or abdominal surgery after informed consent in accordance with our institutional guidelines. This study was approved by the Medical Ethics Review Committee of the Academic Medical Center. Split-skin grafts of 0.3 mm in thickness were obtained using a dermatome (Zimmer). After incubation with Dispase II (1 U ml^{-1}, Roche Diagnostics), epidermal sheets were separated from the dermis and cultured in in Iscoves Modified Dulbeccos's Medium (IMDM, Thermo Fischer Scientific) supplemented with 10% FCS, gentamycine (20 μg ml^{-1}, Centrafarm), pencilline/streptomycin (10 U ml^{-1} and 10 μg ml^{-1}, respectively; Invitrogen). Further LC purification was performed using a Ficoll gradient (Axis-shield) and CD1a microbeads (Miltenyl Biotec) as described before[4,10]. Isolated LCs were routinely 90% pure and expressed high levels of Langerin and CD1a. MUTZ-LCs were differentiated from $CD34^+$ human AML cell line MUTZ3 progenitors in the presence of GM-CSF (100 ng ml^{-1}, Invitrogen), TGF-β (10 ng ml^{-1}, R&D) and TNF-α (2.5 ng ml^{-1}, R&D) and cultured as described before[14]. Immature DCs were differentiated from monocytes, isolated from buffy coats of healthy volunteer blood donors (Sanquin, The Netherlands), in the presence of IL-4 (500 U ml^{-1}, Invitrogen) and GM-CSF (800 U ml^{-1}, Invitrogen) and used at day 6 or 7 as previously described[20]. $CD4^+$ T cells were obtained from peripheral blood mononuclear cells (PBMCs) activated with phytohaemagglutinin (1 mg ml^{-1}; L2769, Sigma Aldrich) for 3 days, enriched for $CD4^+$ T cells by negative selection using MACS beads (130-096-533, Miltenyi) and cultured overnight with IL-2 (20 U ml^{-1}; 130-097-745, Miltenyi) as described before[5]. The following inhibitors were used: rapamycin (mTOR inhibitor, tlrl-rap, Invivogen), bafilomycin A1 (V-ATPase inhibitor; tlrl-baf1; Invivogen) and MG-132 (proteasome inhibitor; 474790; Calbiochem).

Plasmids and cell lines. All cell lines were obtained from ATCC and tested negative for mycoplasma contamination, determined in 3-day-old cell cultures by PCR. Langerin and Langerin mutant W264R expression plasmid pcDNA3.1 were obtained from Life Technologies and subcloned into lentiviral construct pWPXLd (Addgene). HIV-1-based lentiviruses were produced by co-transfection of 293T cells with the lentiviral vector construct, the packaging construct (psPAX2, Addgene) and vesicular stomatitis virus glycoprotein envelope (pMD2.G, Addgene) as described previously[31]. U87 cell lines stably expressing CD4 and wild-type CCR5 co-receptor (obtained through the NIH AIDS Reagent Program, Division of AIDS, NIAID, NIH: U87 $CD4^+CCR5^+$ cells from H. K. Deng and D. R. Littman[32]) were transduced with HIV-1-based lentiviruses expressing sequences coding human TRIM5α[33], rhesus TRIM5α[33], wild-type Langerin or Langerin(W264R).

Viruses, HIV-1 infection and transmission. NL4.3, NL4.3-BaL, SF162, NL4.3eGFP-BaL, NL4.3-BlaM-Vpr and VSV-G-pseudotyped NL4.3(ΔEnv) HIV-1 were generated as described[10]. All produced viruses were quantified by p24 ELISA (Perkin Elmer Life Sciences) and titrated using the indicator cells TZM-Bl. Primary LCs and MUTZ-LCs were infected with a multiplicity of infection of 0.2–0.4 and HIV-1 infection was assessed by flow cytometry at day 7 after infection by intracellular p24 staining. Double staining with CD1a (LCs marker; HI149-APC; BD Pharmigen) and p24 (KC57-RD1-PE; Beckman Coulter) was used to discriminate the percentage of $CD1a^+p24^+$ infected LCs. $CD4^+CCR5^+$ U87 parental or transduced cells were infected at a multiplicity of infection of 0.1–0.2 and HIV-1 infection was assessed at day 3 after infection by intracellular p24 staining or GFP expression. For analysis of transmission of HIV-1 to T cells, LCs were stringently washed 3 days after infection followed by co-culture with activated allogeneic $CD4^+$ T cells for 3 days. Triple staining with CD1a (LCs marker), CD3 (T cells marker; 552851-PercP, BD Pharmigen) and p24 was used to discriminate the percentage of $CD3^+CD1a^-p24^+$ infected T cells. HIV-1 infection and transmission was assessed by FACSCanto II flow cytometer (BD Biosciences) and data analysis was carried out with FlowJo software (Treestar). HIV-1 production was determined by a p24 antigen ELISA in culture supernatants (ZeptoMetrix).

RNA isolation and quantitative real-time PCR. mRNA was isolated with an mRNA Capture kit (Roche) and cDNA was synthesized with a reverse-transcriptase kit (Promega). For real-time PCR analysis, PCR amplification was performed in the presence of SYBR green in a 7500 Fast Realtime PCR System (ABI). Specific primers were designed with Primer Express 2.0 (Applied Biosystems; Extended Data Table 1). The cycling threshold (C_t) value is defined as the number of PCR cycles in which the fluorescence signal exceeds the detection threshold value. For each sample, the normalized amount of target mRNA (N_t) was calculated from the C_t values obtained for both target and household (GAPDH, primary LCs, DCs and U87 cells lines; β-actin, MUTZ-LCs) mRNA with the equation $N_t = 2^{Ct(control) - Ct(target)}$. For relative mRNA expression, control siRNA sample was set at 1 within the experiment and for each donor.

HIV-1 integration Alu-PCR assay. A two-step Alu-long terminal repeat (LTR) PCR was used to quantify the integrated HIV-1 DNA in infected cells as previously described[20]. Total cell DNA was isolated at 16 h after infection (multiplicity of infection of 0.4) with a QIAamp blood isolation kit (Qiagen). In the first round of PCR, the DNA sequence between HIV-1 LTR (LTR R region, extended with a marker region at the 5′ end) and the nearest Alu repeat was amplified (primer sequences, Extended Data Table 1). The second round was nested quantitative real-time PCR of the first-round PCR products using primers annealing to the aforementioned marker region in combination with another HIV-1-specific primer (LTR U5 region) by real-time quantitative PCR. Two different dilutions of the PCR products from the first-round of PCR were assayed to ensure that PCR inhibitors were absent. For monitoring the signal contributed by unintegrated HIV-1 DNA, the first-round PCR was also performed using the HIV-1-specific primer (LTR R region) only. HIV-1 integration was normalized relative to GAPDH DNA levels. For relative HIV-1 integration, control siRNA-infected cells (total signal; Supplementary Table 1) was set as 1 for one experiment or for each donor.

HIV-1 fusion assay. A BlaM-Vpr-based assay was used to quantify fusion of HIV-1 to the host membrane in infected LCs as previously described[10]. LCs were infected with NL4.3-BlaM-Vpr for 2 h and then loaded with CCF2/AM (1 mM, LiveBLAzer FRET-B/G Loading Kit, Life technologies) in serum-free IMDM medium for 1 h at 25 °C. After washing, BlaM reaction was allowed to develop for 16 h at 22 °C in IMDM supplemented with 10% FCS and 2.5 mM anion transport inhibitor probenecid (Sigma Pharmaceuticals). HIV-1 fusion was determined by monitoring the changes in fluorescence of CCF2/AM dye, which reflect the presence of BlaM-Vpr into the cytoplasm of target cells upon viral fusion. The shift from green emission fluorescence (500 nm) to blue emission fluorescence (450 nm) of CCF2/AM dye was assessed by flow cytometer LSRFortessa (BD Biosciences) and data analysis was carried out with FlowJo software. Percentages of blue fluorescent $CCF2/AM^+$ cells are depicted as percentage of HIV-1 fusion.

HIV-1 binding assay. A fluorescent bead adhesion assay was used to examine the ability of HIV-1 gp120-coated fluorescent beads to bind Langerin in $CD4^+CCR5^+$ U87 transfectants as previously described[5]. Binding was measured by FACSCanto II flow cytometer and data analysis was carried out with FlowJo software.

RNA interference. Skin LCs and DCs were transfected with 50 nm siRNA with the transfection reagent DF4 (Dharmacon) whereas MUTZ-LCs, $CD4^+CCR5^+$ U87 parental or transduced cells were transfected with transfection reagent DF1 (Dharmacon) and were used for experiments 48–72 h after transfection. The siRNA (SMARTpool; Dharmacon) were specific for Atg5, (M-004374-04), Atg16L1 (M-021033), LSP-1 (M-012640-00), TRIM5α (M-007100-00) and non-targeting siRNA (D-001206-13) served as control. Langerin was silenced in MUTZ-LCs by electroporation with Neon Transfection System (ThermoFischer Scientific) using siRNA Langerin (10 μM siRNA, M-013059-01, SMARTpool; Dharmacon). Silencing of the aforementioned targets was verified by real-time PCR, flow cytometer and immunoblotting (Extended Data Figs 1d, e, 2a–k).

Intracellular staining of LC3 II. Cells were pre-treated with bafilomycin A1 for 2 h or left untreated followed by incubation with HIV-1 for 16 h. Quantification of intracellular LC3 II levels by saponin extraction was performed as described before[34,35]. LCs were washed in PBS and permeabilized with 0.05% saponin in PBS. Cells were incubated at 4 °C for 30 min with mouse anti-LC3 primary antibody (M152-3; MBL International) or with mouse anti-IgG1 isotype control (MOPC-21; BD Pharmingen) followed by incubation with Alexa Fluor 488-conjugated goat-anti mouse IgG_1 antibody (A-21121, Life Technologies) in saponin buffer. Intracellular LC3 II levels were assessed by FACSScan or FACSCanto II flow cytometers (BD Biosciences) and data analysis was carried out with FlowJo.

Immunoblotting for LC3. Cells were pre-treated with bafilomycin for 2 h or left untreated followed by incubation with HIV-1 for 4 h. Quantification of intracellular LC3 II levels by saponin extraction was performed as described before[35]. Whole-cell extracts were prepared using RIPA lysis buffer supplemented with protease inhibitors (9806; Cell Signalling). 20–30 μg of extract were resolved by SDS–PAGE (15%) and immunoblotted with LC3 (2G6; Nanotools) and β-actin (sc-81178; Santa Cruz) antibodies, followed by incubation with HRP-conjugated secondary rabbit-anti-mouse antibody (P0161; Dako) and luminol-based enhanced chemiluminescence (ECL) detection (34075; Thermo Scientific). For gel source data, see Supplementary Fig. 1.

Electron microscopy. MUTZ-LCs (2×10^6) were incubated for 16 h with HIV-1 NL4.3 (multiplicity of infection, 0.5) or left untreated as a control, fixed in 4% paraformaldehyde and 1% glutaraldehyde in sodium cacodylate buffer for 10 min at room temperature followed by 24 h at 4 °C. After fixation, cells were collected by centrifugation and the pellet was washed in sodium cacodylate buffer. Cells were post-fixed for 1 h at 4 °C (1% osmium tetroxide, 0.8% potassium ferrocyanide in the same buffer), contrasted in 0.5% uranyl acetate, dehydrated in a graded ethanol series and embedded in epon LX112. Ultrathin sections were stained with uranylacetate/lead citrate and examined with a FEI Tecnai-12 transmission electron

microscope. Numbers of autophagosomes per cell was determined in 50 cells for each condition counted by two independent researchers.

Confocal microscopy. LCs were left to adhere onto poly-L-lysine coated slides. Cells were fixed in 4% paraformaldehyde and permeabilized with PBS/0.1% saponin/1% BSA/1 mM Hepes. Cells were stained with anti-Langerin (AF2088; R&D Systems) and TRIM5α (ab109709; Abcam) antibodies followed by Alexa Fluor 647-conjugated anti-goat (A-21447; Life Technologies) and Alexa Fluor 488-conjugated anti-rabbit (A-21206; Life Technologies). For detection of autophagic vesicles, LCs were pre-loaded with the Cyto-ID Green detection autophagy reagent (ENZ-51031; Enzo Life Sciences), which was previously shown to specifically stain autophagic vesicles[36] before adherence to microscope slides and stained with p24 (KC57-RD1-PE; Beckman Coulter) followed by Alexa-Fluor-546-conjugated anti-mouse (A-11003; Life Technologies). Nuclei were counterstained with Hoechst (10 μg ml^{-1}; Molecular Probes). Single plane images were obtained by Leica TCS SP-8 X confocal microscope and data analysis was carried out with Leica LAS AF Lite (Leica Microsystems).

Immunoprecipitation and immunoblotting. Whole-cell extracts were prepared using RIPA lysis buffer supplemented with protease inhibitors. Atg16L1, DC-SIGN, Langerin, p62 and TRIM5α were immunoprecipitated from 40 μg of extract with anti- Atg16L1 (PM040; MBL International), DC-SIGN (AZN-D1)[19], Langerin (10E2)[5], p62 (ab56416; Abcam), TRIM5α (ab109709; Abcam), mouse IgG1 isotype control (MOPC-21; BD Pharmingen), mouse IgG2a isotype control (IC003A; R&D systems) and rabbit IgG control (sc-2077; Santa Cruz) coated on protein A/G PLUS agarose beads (sc-2003; Santa Cruz), washed twice with ice-cold RIPA lysis buffer and resuspended in Laemmli sample buffer (161-0747, Bio-Rad). Immunoprecipitated samples were resolved by SDS–PAGE (12.5%), and detected by immunoblotting with Atg5 (PM050; MBL), Atg16L1 (MBL), DC-SIGN (551186; BD Biosciences), Langerin (AF2088; R&D Systems), LSP-1 (3812S; Cell Signalling), TRIM5α (Abcam) and HIV-p24 (KC57-RD1-PE; Beckman Coulter) antibodies, followed by incubation with Clean-Blot IP Detection Kit-HRP (21232; Thermo Scientific) and ECL detection (34075; Thermo Scientific). Data acquisition was carried out with ImageQuant LAS 4000 (GE Healthcare). Immunoprecipitation with TRIM5α, Langerin, DC-SIGN, Atg16L1 and p62 pulls-down mostly the TRIM5α (approximately 56 kDa) form. Relative intensity of the bands was quantified using Image Studio Lite 5.2 software by normalizing β-actin and set at 1 in untreated cells. For gel source data, see Supplementary Fig. 1.

Statistical analysis. Two-tailed Student's *t*-test for paired observations (differences of stimulations within the same donor or cell-type) or unpaired observation (differences between U87 transfectants). Statistical analyses were performed using GraphPad 6.0 software and significance was set at $P < 0.05$ ($^{*}P < 0.05$; $^{**}P < 0.01$).

Data availability. The data that support the findings of this study are available from the corresponding author upon reasonable request.

31. Arrighi, J. F. *et al.* DC-SIGN-mediated infectious synapse formation enhances X4 HIV-1 transmission from dendritic cells to T cells. *J. Exp. Med.* **200,** 1279–1288 (2004).
32. Björndal, A. *et al.* Coreceptor usage of primary human immunodeficiency virus type 1 isolates varies according to biological phenotype. *J. Virol.* **71,** 7478–7487 (1997).
33. Setiawan, L. C. & Kootstra, N. A. Adaptation of HIV-1 to rhTrim5α-mediated restriction *in vitro*. *Virology* **486,** 239–247 (2015).
34. Eng, K. E., Panas, M. D., Karlsson Hedestam, G. B. & McInerney, G. M. A novel quantitative flow cytometry-based assay for autophagy. *Autophagy* **6,** 634–641 (2010).
35. Klionsky, D. J. *et al.* Guidelines for the use and interpretation of assays for monitoring autophagy. *Autophagy* **8,** 445–544 (2012).
36. Chan, L. L. *et al.* A novel image-based cytometry method for autophagy detection in living cells. *Autophagy* **8,** 1371–1382 (2012).

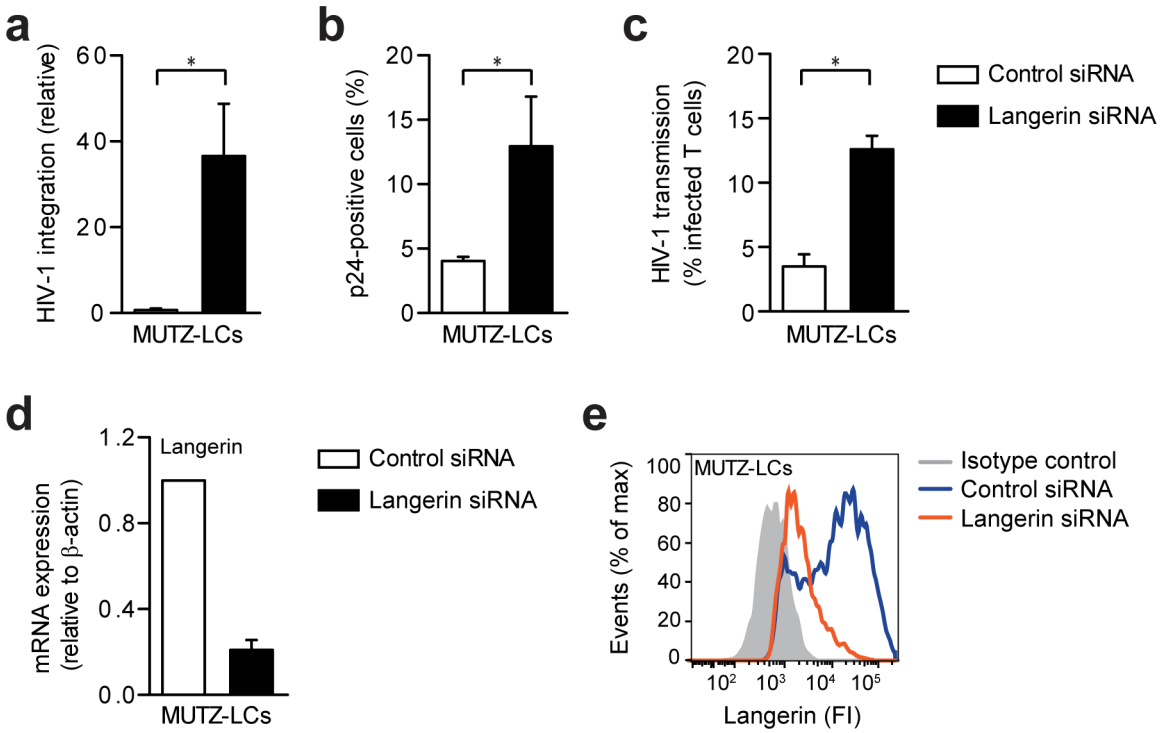

Extended Data Figure 1 | Langerin in MUTZ-LCs restricts HIV-1 integration, infection and transmission to CD4$^+$ T cells. a, **b**, HIV-$1_{NL4.3}$ integration (**a**) and infection (**b**) of MUTZ-LCs after Langerin silencing, determined by Alu-PCR (**a**) and intracellular p24 staining (**b**). **c**, HIV-$1_{NL4.3\text{-}BaL}$ transmission by MUTZ-LCs after Langerin silencing, determined in LC and T-cell coculture by intracellular p24 staining. **d**, **e**, Silencing was confirmed by real-time PCR (**d**) or by flow cytometer (**e**; representative of $n = 3$). mRNA expression was normalized to β-actin (**d**) and set at 1 in control-siRNA treated cells. *$P < 0.05$ (two-tailed *t*-test). Data are mean ± s.d. of three (**a**, **c**, **d**) and four (**b**) independent experiments.

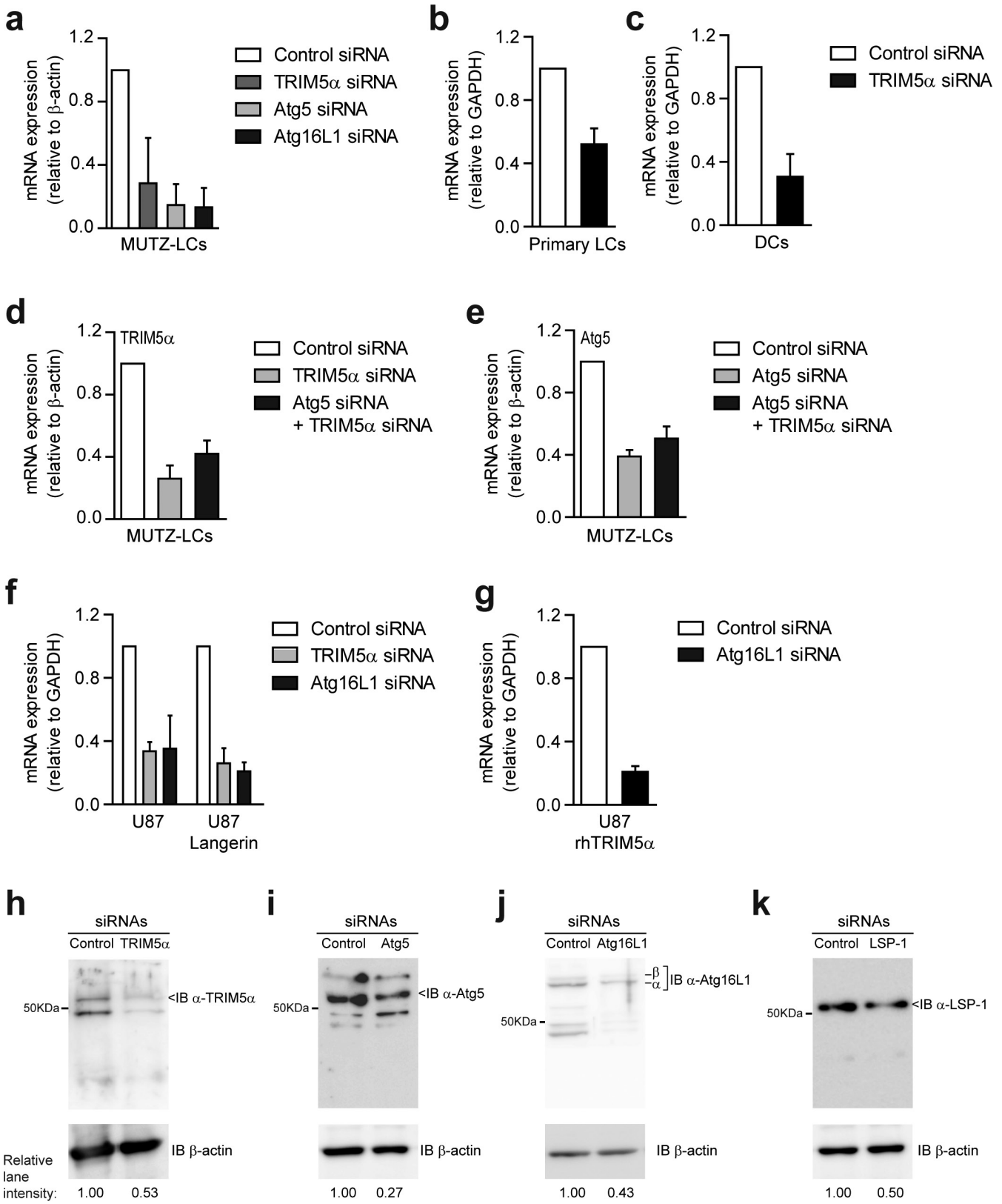

Extended Data Figure 2 | Silencing of TRIM5α, Atg5, Atg16L1 and LSP-1 by RNA interference. a–k, Indicated proteins were silenced using specific SMARTpools and non-targeting siRNA as a control. Silencing was confirmed by real-time PCR (**a–g**) or by immunoblotting (β-actin served as loading control; **h–k**) in MUTZ-LCs (**a**, **d**, **e**, **h**, **i**, **j**), primary LCs (**b**), DCs (**c**), $CD4^+CCR5^+$ U87 parental cells (**f**) or $CD4^+CCR5^+$ U87 cells transduced with either Langerin (**f**, **k**) or rhesus TRIM5α (**g**). mRNA expression was normalized to β-actin (**a**, **d**, **e**) or GAPDH (**b**, **c**, **f**, **g**) and set at 1 in cells treated with control siRNA. Relative abundance of indicated proteins was quantified by normalizing to β-actin and set at 1 in control siRNA treated cells. Representative of $n = 2$ (**d**, **e**, **h–k**). For gel source data, see Supplementary Fig. 1. Data are mean ± s.d. of three (**a**, **c**, **f**, **g**) and six (**b**) independent experiments.

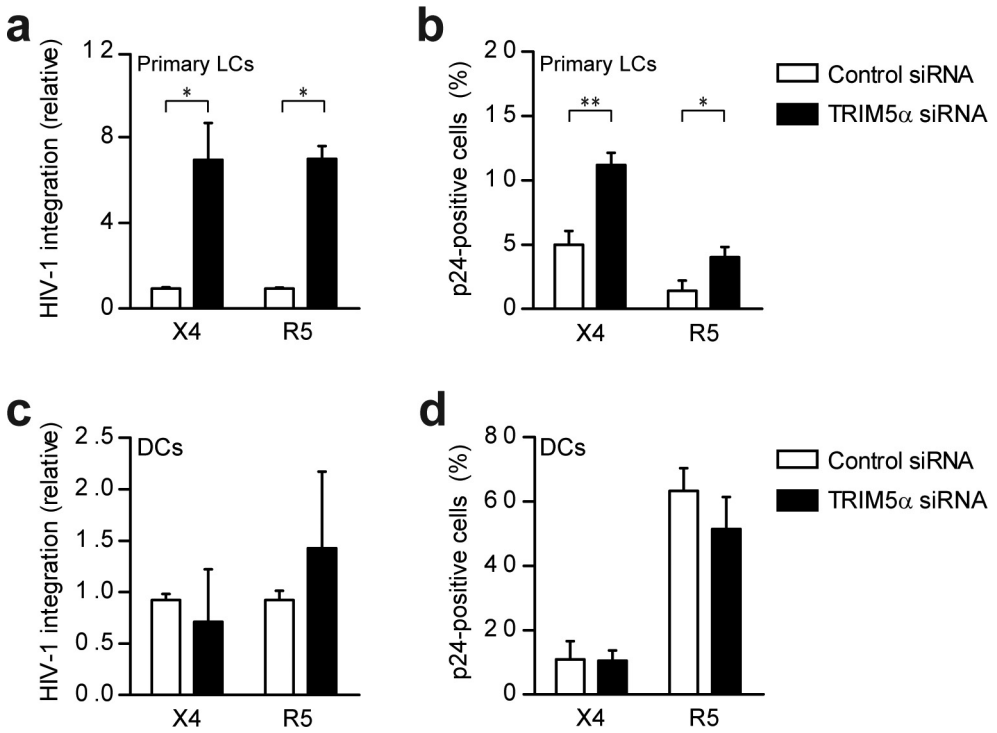

Extended Data Figure 3 | Human TRIM5α-mediated restriction in LCs or, the lack thereof in DCs, is independent of virus tropism. a–d, HIV-$1_{NL4.3}$ (X4, CXCR4-tropic virus) or HIV-$1_{NL4.3\text{-}BaL}$ (R5, CCR5-tropic virus) integration (**a**, **c**) and infection (**b**, **d**) of primary LCs (**a**, **b**) or DCs (**b**, **d**) after TRIM5α silencing determined by Alu-PCR (**a**, **c**) and intracellular p24 staining (**b**, **d**). $^*P < 0.05$, $^{**}P < 0.01$ (two-tailed *t*-test). Data are mean ± s.d. of three (**a–d**) independent experiments.

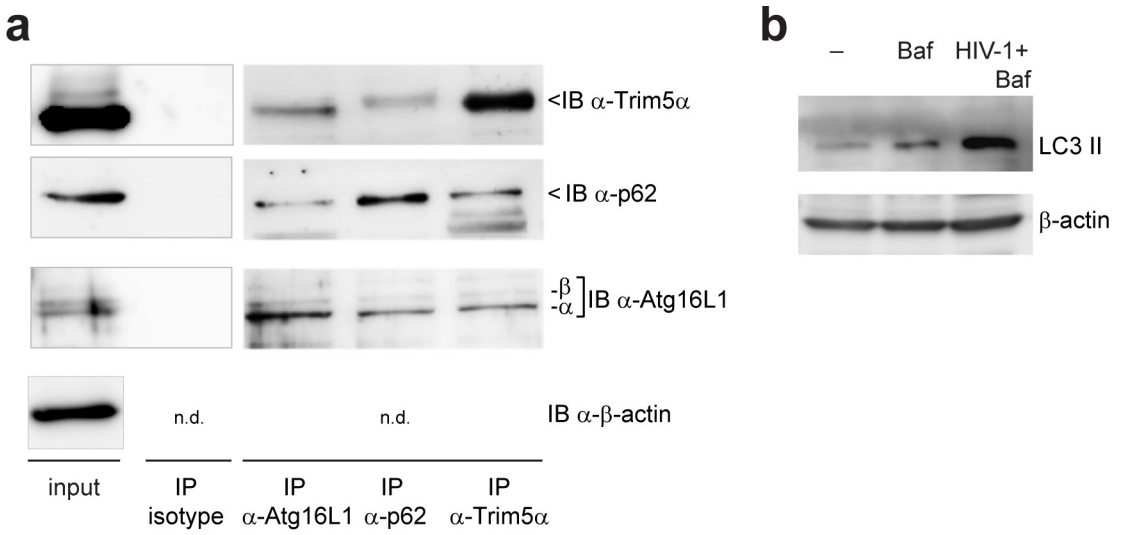

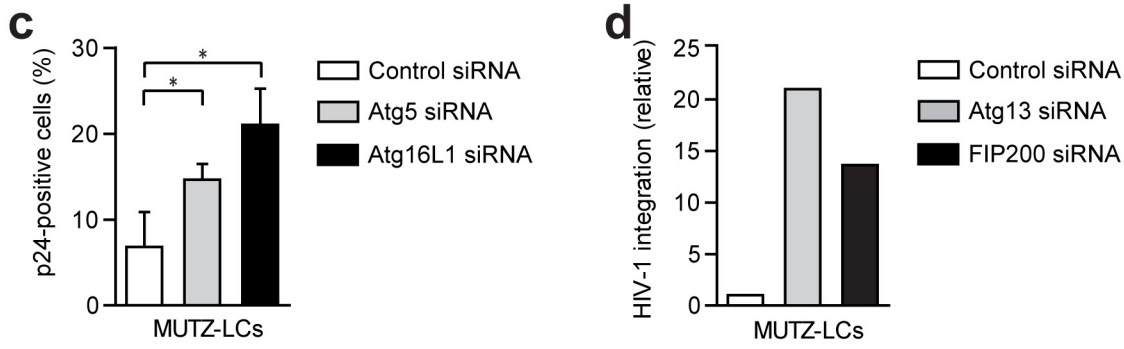

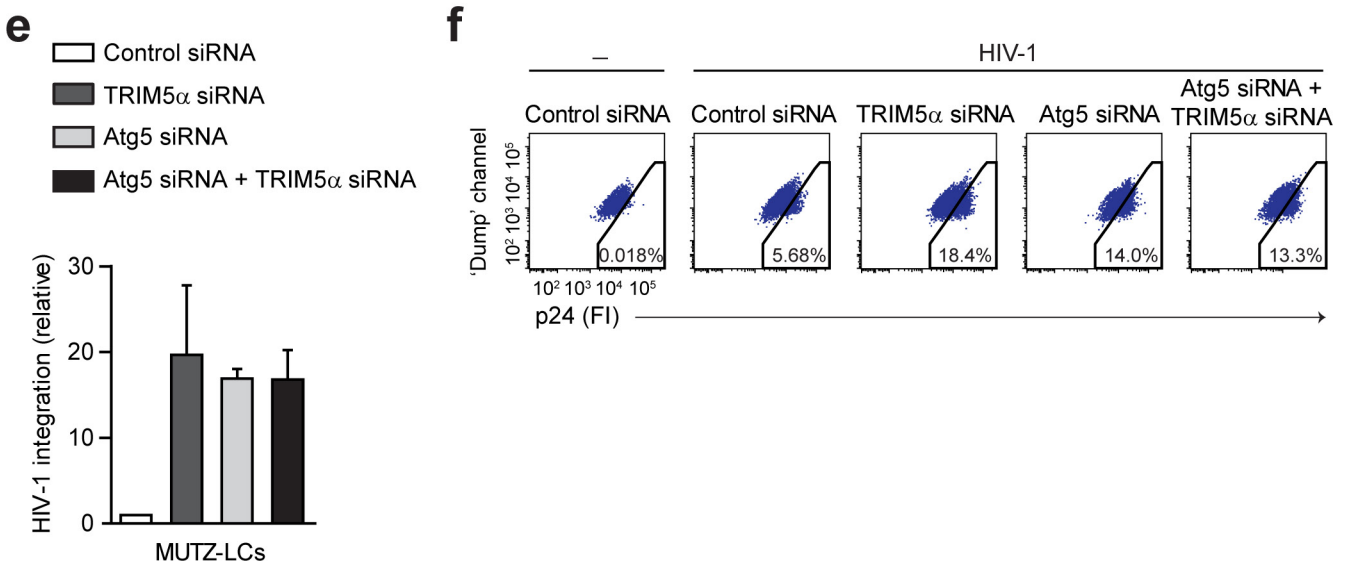

Extended Data Figure 4 | ULK1 complex-dependent autophagy restricts HIV-1 integration in LCs and human TRIM5α restriction is dependent on Atg5 function. a, TRIM5α, p62 and Atg16L1 in whole-cell lysates of uninfected MUTZ-LCs before (input) or after immunoprecipitation with Atg16L1, p62, TRIM5α, rabbit IgG control (as control for Atg16L1 and TRIM5α IP) or mouse IgG2a isotype control (as control for p62 immunoprecipitation), determined by immunoblotting (n.d., not determined). **b**, Autophagy induction in primary LCs pre-treated with bafilomycin followed by incubation with HIV-$1_{NL4.3}$, determined by immunoblotting for LC3. For gel source data, see Supplementary Fig. 1. **c**, HIV-$1_{NL4.3}$ infection of MUTZ-LCs after Atg5 or Atg16L1 silencing, determined by intracellular p24 staining. **d**, HIV-$1_{NL4.3}$ integration into MUTZ-LCs after Atg13 or FIP200 silencing, determined by Alu-PCR. **e**, **f**, HIV-$1_{NL4.3}$ integration (**e**) or infection (**f**) of MUTZ-LCs after Atg5, TRIM5α silencing or simultaneously with Atg5 and TRIM5α silencing, determined by Alu-PCR (**e**) and intracellular p24 staining (**f**). Data are representative of three (**a**) or two (**b**, **d**–**f**) experiments and mean ± s.d. of four independent experiments (**c**).

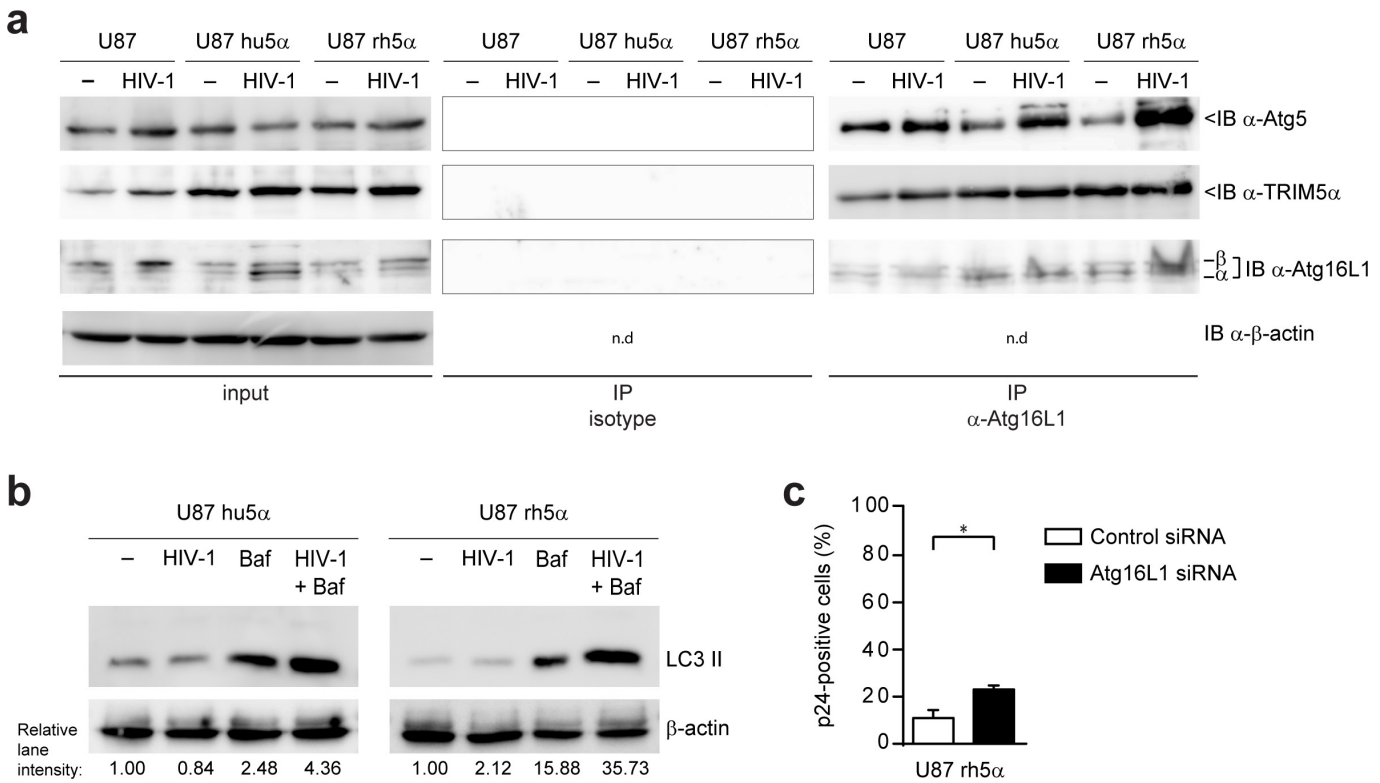

Extended Data Figure 5 | Increased Atg5 recruitment into TRIM5α–Atg16L1 complex scaffold in CD4$^+$CCR5$^+$ U87 transfectants. a, Atg5, TRIM5α and Atg16L1 in whole-cell lysates of CD4$^+$CCR5$^+$ U87 parental cells (U87) or transduced with either human TRIM5α (U87 hu5α) or rhesus TRIM5α (U87 rh5α) infected with HIV-$1_{NL4.3\text{-}BaL}$ before (input) or after immunoprecipitation with Atg16L1 or rabbit IgG control, determined by immunoblotting (n.d., not determined). **b**, Autophagy induction in U87 transfectants with bafilomycin followed by incubation with HIV-1_{SF162}, determined by immunoblotting for LC3 (autophagy induction in control CD4$^+$CCR5$^+$ U87 parental cells presented in Fig. 3o). Relative abundance of LC3 II determined by normalizing to β-actin. Representative of $n = 2$ (**a**, **b**). For gel source data, see Supplementary Fig. 1. **c**, HIV-1_{SF162} infection of CD4$^+$CD5$^+$ U87 cells transduced with rhesus TRIM5α after Atg16L1 silencing, determined by intracellular p24 staining. *$P < 0.05$ (t-test). Data are mean ± s.d. of three (**c**) independent experiments.

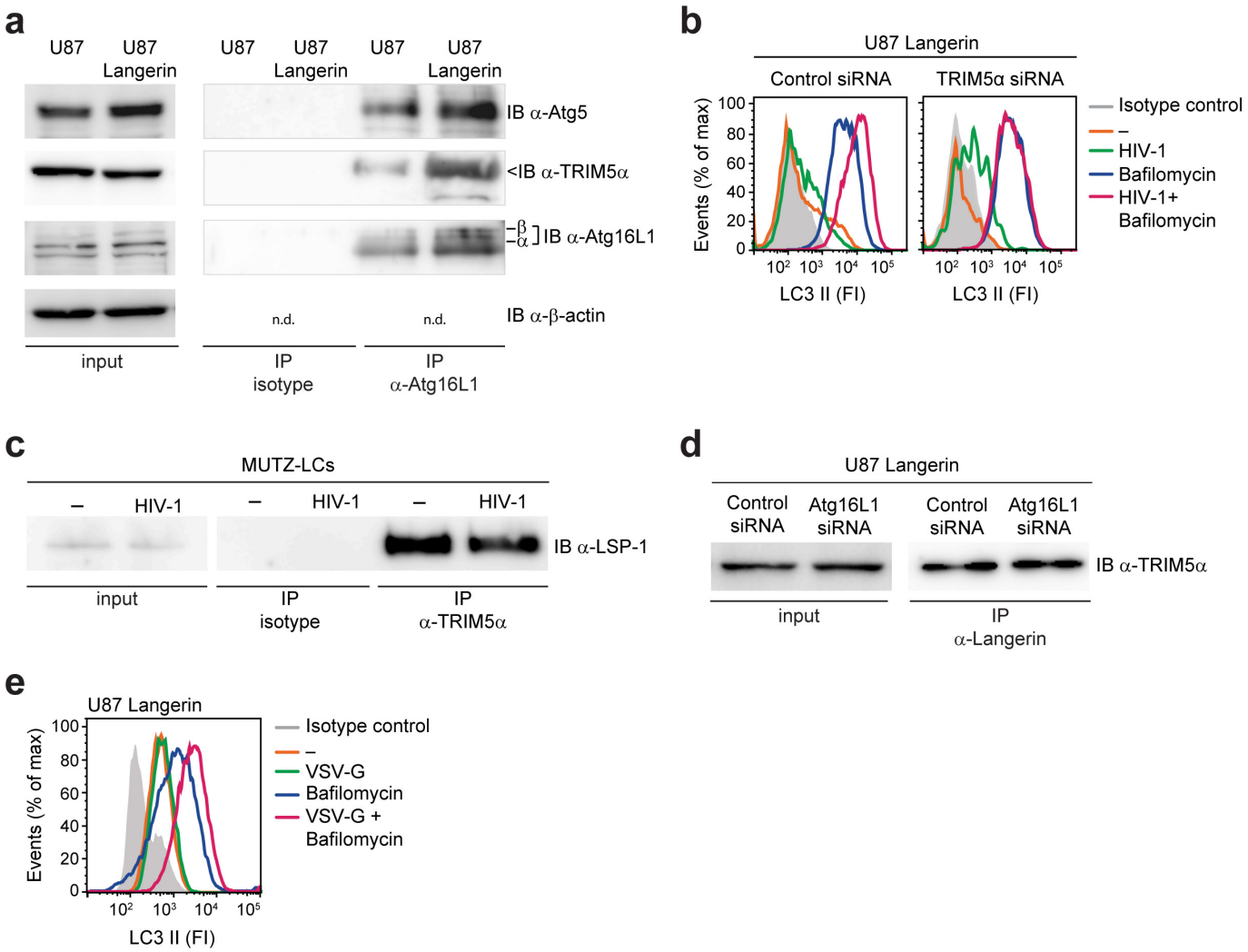

Extended Data Figure 6 | Human TRIM5α induces autophagy upon HIV-1 exposure in Langerin$^+$ U87 transfectant and interacts with Langerin through LSP-1, but not Atg16L1. a, Atg5, TRIM5α and Atg16L1 in whole-cell lysates of CD4$^+$CCR5$^+$ U87 parental cells (U87) or transduced with Langerin (U87 Langerin) before (input) or after immunoprecipitation with Atg16L1 or rabbit IgG control, determined by immunoblotting (n.d., not determined). **b**, Autophagy levels in Langerin$^+$ U87 transfectant after TRIM5α silencing, pre-treated with bafilomycin followed by incubation with HIV-$1_{NL4.3\text{-}BaL}$, determined by intracellular LC3 II levels by flow cytometer. **c**, LSP-1 in whole-cell lysates of MUTZ-LCs infected with HIV-$1_{NL4.3}$ before (input) or after immunoprecipitation with TRIM5α or rabbit IgG control. **d**, TRIM5α in whole-cell lysates of Langerin$^+$ U87 transfectant after Atg16L1 silencing before (input) or after immunoprecipitation with Langerin, determined by immunoblotting. For gel source data, see Supplementary Fig. 1. **e**, Autophagy induction in Langerin$^+$ U87 transfectant pre-treated with bafilomycin followed by incubation with VSV-G-pseudotyped HIV-1, determined by intracellular LC3 II levels. Data are representative of two experiments (**a**–**e**).

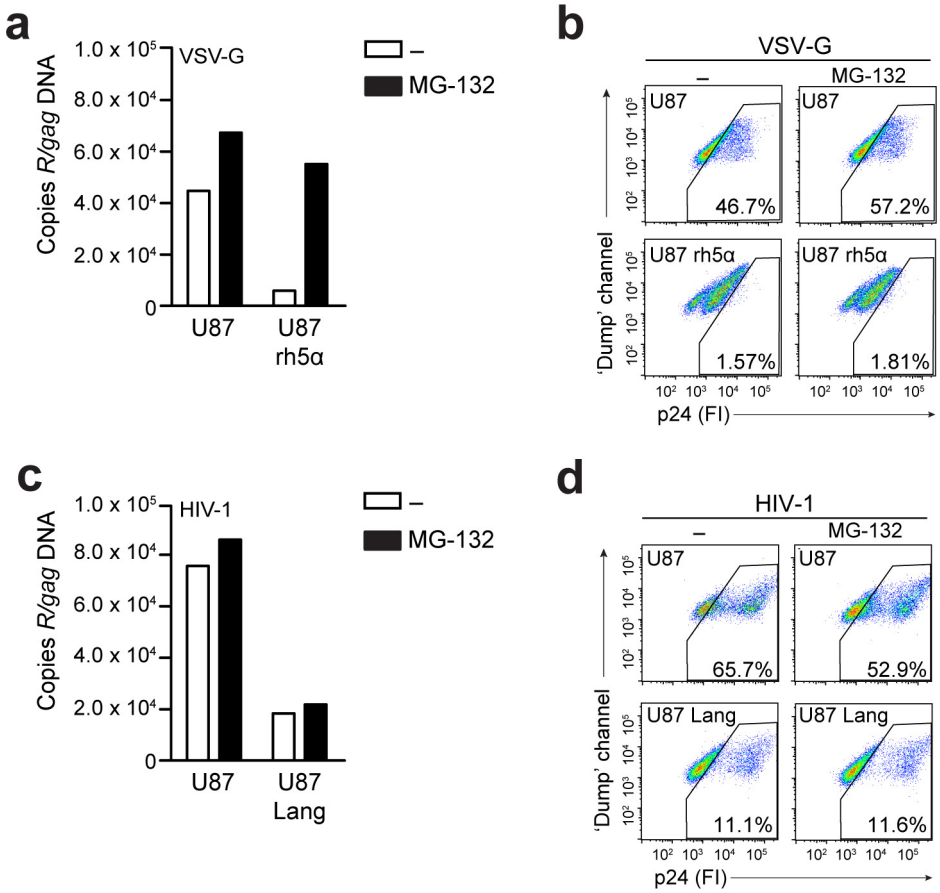

Extended Data Figure 7 | Proteosome inhibition does not relieve Langerin-mediated restriction of HIV-1 reverse-transcription products nor infection. a–d, *R/gag* proviral DNA levels (**a**, **c**) and HIV-1 infection (**b**, **d**) in $CD4^+CCR5^+$ U87 parental cells (U87) or cells transduced with either rhesus TRIM5α (U87 rh5α) or Langerin (U87 Lang) after pre-treatment with proteosome inhibitor MG-132 and infected with VSV-G-pseudotyped HIV-1 (**a**, **b**; VSV-G) or HIV-$1_{NL4.3\text{-}BaL}$ (**c**, **d**; HIV-1), determined by qPCR (**a**, **c**) and intracellular p24 staining (**b**, **d**). Data are representative of two experiments (**a–d**).

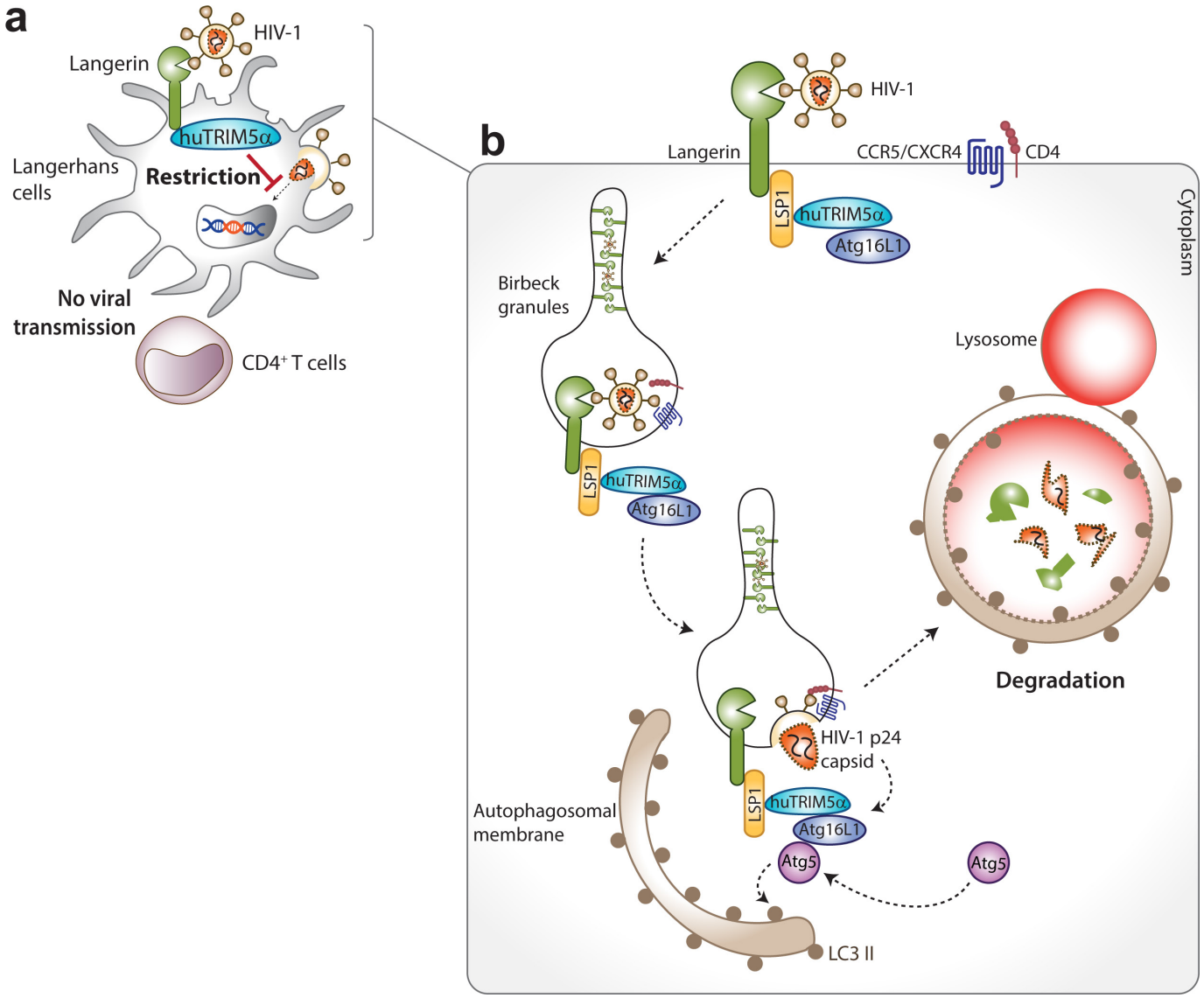

Extended Data Figure 8 | Langerin-controlled human TRIM5α restriction mechanism in Langerhans cells. a, HIV-1 binding to Langerin in Langerhans cells drives human TRIM5α-mediated restriction of viral integration, HIV-1 infection and HIV-1 transmission to $CD4^+$ T cells. **b**, Langerin associates at steady-state with LSP-1–TRIM5α–Atg16L1 complex. Capture of HIV-1 by Langerin targets internalization of the incoming virus into Birbeck granules. Upon viral fusion, human TRIM5α mediates recruitment of Atg5 to TRIM5α–Atg16L1–HIV-1p24 capsid complex, which promotes lipidation of LC3 (LC3 II) and thereby elicit autophagosome formation. Vesicles containing Langerin–HIV-1 capsid complexes are subsequently targeted into autophagosomes for lysosomal degradation, which prevents infection of Langerhans cells.

Extended Data Table 1 | Primer sequences used for mRNA expression and HIV-1 integration assay

mRNA expression primer sequences

Gene product	Forward primer	Reverse primer
Atg5	TCATTCAGAAGCTGTTTCGTCC	CCCCATCTTCAGGATCAATAGC
Atg16L1	TGCTCCCGTGATGACTTGC	CAACTCTGGTCCAGTCAGAGCC
TRIM5α	AGAACATACGGCCTAATCGGC	CAACTTGACCTCCCTGAGCTTC
GAPDH	CCATGTTCGTCATGGGTGTG	GGTGCTAAGCAGTTGGTGGTG
β-actin	GCTCCTCCTGAGCGCAAG	CATCTGCTGGAAGGTGGACA

HIV-1 integration primer sequences

Primer	Primer sequence
HIV-1 LTR R* (forward)	ATGCCACGTAAGCGAAACTGCTGGCTAACTAGGGAACCCACTG
Alu (reverse)	TCCCAGCTACTGGGGAGGCTGAGG
Second-round marker (forward)	ATGCCACGTAAGCGAAACTG
HIV-1 LTR U5 (reverse)	CACACTGACTAAAAGGGTCTGAGG
GAPDH DNA (forward)	TACTAGCGGTTTTACGGGCG
GAPDH DNA (reverse)	TCGAACAGGAGGAGCAGAGAGCGA

*Marker sequence at 5′ end underlined.